Chemical Mapping of Paleontological and Archeological Artifacts with Synchrotron X-Rays

Uwe Bergmann,[1] Phillip L. Manning,[2] and Roy A. Wogelius[2]

[1]Linac Coherent Light Source, SLAC National Accelerator Laboratory, Menlo Park, California 94025; email: bergmann@slac.stanford.edu

[2]Williamson Research Center for Molecular Environmental Science, School of Earth, Atmospheric, and Environmental Sciences, University of Manchester, Manchester M13 9PL, United Kingdom; email: phil.manning@manchester.ac.uk, roy.wogelius@manchester.ac.uk

Annu. Rev. Anal. Chem. 2012. 5:361–89

First published online as a Review in Advance on April 9, 2012

The *Annual Review of Analytical Chemistry* is online at anchem.annualreviews.org

This article's doi: 10.1146/annurev-anchem-062011-143019

1936-1327/12/0719-0361$20.00

Keywords

X-ray fluorescence, imaging, X-ray absorption, infrared, fossil, taphonomy

Abstract

The application of the recently developed synchrotron rapid scanning X-ray fluorescence (SRS-XRF) technique to the mapping of large objects is the focus of this review. We discuss the advantages of SRS-XRF over traditional systems and the use of other synchrotron radiation (SR) techniques to provide corroborating spectroscopic and diffraction analyses during the same analytical session. After reviewing routine techniques used to analyze precious specimens, we present several case studies that show how SR-based methods have been successfully applied in archeology and paleontology. For example, SRS-XRF imaging of a seventh-century Qur'ān palimpsest and an overpainted original opera score from Luigi Cherubini is described. We also review the recent discovery of soft-tissue residue in fossils of *Archaeopteryx* and an ancient reptile, as well as work that has successfully resolved the remnants of pigment in *Confuciusornis sanctus*, a 120-million-year-old fossil of the oldest documented bird with a fully derived avian beak.

1. INTRODUCTION TO THE CHEMICAL ANALYSIS OF ANCIENT ARTIFACTS AND FOSSILS

Chemistry can define the origins, synthesis, function, and subsequent alterations and modifications of both inorganic and organically derived molecules. Infrared (IR) spectroscopy– and synchrotron-based X-ray analyses have recently been successfully used in the fields of archeology and paleontology (1–15). Detailed knowledge of the chemical composition (both inorganic and organic) of archeological objects, as well as of plants and animals (both extant and extinct), can unlock crucial information to aid in restoration, constrain kinetics of decomposition after burial, and resolve mass transfer of elements between the environment and the object being analyzed. The chemical inventory of an object or the matrix within which it is enclosed can also provide important information about contamination or significant alteration of endogenous compounds (3). The analytical techniques available to detect, resolve, quantify, and map the chemistry of objects may also damage the object under study (2). When samples are rare, limited, or priceless (or, often, a combination of all three), the analytical technique deployed to resolve the chemistry must be carefully considered (2–5, 11).

Archeological studies focus on human artifacts or evidence for the habitation of our species and are usually concerned with subfossil material, in which the processes of mineralization and alteration are limited or absent. Such subfossil material is customarily no older than 30,000 years. Paleontology is concerned with the evidence of past life, ranging from specimens that are 30,000 years old to the first traces of life, which appear in specimens 3.4 billion years old (16). The term fossil is used to describe the remains (both trace and body) of past life; it derives from the Latin fossilis and literally means "something dug up." Trace fossils include tracks, trails, and other traces of biological activity, whereas body fossils include both original and replaced elements of an organism's tissues (bone, chitin, tendon, skin, etc.) (16).

The recognition of both the structure and the composition of fossil soft tissues has been revolutionized by the application of sophisticated new analytical techniques to fossil material; see Schweitzer (17) for a review. The identification of mineralized soft tissue is not restricted to that contained within hard biological materials (e.g., bones and claws). The structure and macromolecular composition of soft tissues, such as dinosaur skin, have also been resolved (1, 16). The suite of techniques available for the study of soft tissue in the fossil record is being extended to IR spectroscopy (1, 2) and synchrotron-based X-ray fluorescence (XRF) (3, 4), yielding new information that could not have been revealed by traditional methods.

We review some of the first results emerging from the application of synchrotron radiation (SR) to produce chemical maps of archeological and paleontological specimens. Before we turn to several case studies, we provide a brief discussion of the aims of such studies and the unique set of problems that they present for analytical chemistry. We then explain how synchrotron methods build on more traditional types of analysis and, finally, describe four case studies that highlight the type of information that can be harvested through the use of synchrotron methods.

1.1. Aims

Detailed chemical analysis of paleontological and archeological specimens has three major aims, which we discuss below.

1.1.1. Restoring lost information. The study of fossil remains and ancient human artifacts provides a wealth of information to a wide range of disciplines. Restoring or uncovering lost information can provide, for example, insight into past cultures or cultural events and, more

generally, can explain how systems or organisms adapted and evolved over time. Such work may also enhance our ability to predict how current systems will evolve in the future; of course, the study of preserved specimens provides one of the few ways in which we can learn how extinct organisms and the worlds they once inhabited may have functioned. Through chemical analysis of such specimens, we can tease out the biochemical and environmental signatures of now-extinct life and the contextual data from past worlds. Fundamental scientific questions may be unequivocally answered by chemical analysis of physical remnants. Piecing together various strands of chemical evidence with other sources of information, such as structural data or knowledge of a specimen's precise age, history, and provenance, can then yield critical insights about a specific event, environment, person, or species. Thus, a key aim of such chemical analyses is to restore, to the greatest extent possible, lost information from the material being studied.

1.1.2. Understanding the aging process. There are, of course, subsidiary aims in these types of studies. In some cases, it is important to understand the process of aging (often over vast geologic timescales) itself, and chemical analysis may provide useful information about reaction pathways, rates, and controlling variables. For example, in paleontology, the complex set of chemical and structural changes that may affect a specimen once it has been buried is referred to as taphonomy (literally, "burial laws") (16). The taphonomic processes might be completely different for two identical organisms buried at the same time but in environments that were chemically very different (with associated variability in sedimentary matrices and pore-water chemistry). Likewise, the burial history of archeological objects can be strongly controlled by the ambient chemical conditions and the prevailing environment (often linked to climate, rapidity of burial, etc.). Improving our understanding of how materials alter and sometimes degrade over long periods of elapsed time allows us to directly compare specimens that have experienced different taphonomic conditions (3). The geological history of a discrete package of sediment might also yield important information about the depth and duration of deep burial, which has a major impact on the chemistry of groundwater and the formation of specific mineral types (1). Two formations of identical age, environment and faunal/floral composition, might look very different as a function of the geologic aging processes that can affect a group of successive geological strata (i.e., a succession of sediments laid down and subsequently lithified). Therefore, understanding the various processes of aging is an important and often overlooked aim of this type of research.

1.1.3. Predicting chemical pathways in similar objects. Finally, because detailed chemical information can teach us about the key variables that control and/or influence degradation, such information can enable us to make predictions about degradation rates and pathways for a range of materials. Doing so enhances our predictive capacity, leads us to make better sampling choices, helps us to design improved curatorial strategies, and has direct effects on other fields in which long-term phase stability is desired. The chemical inventory of a fossil or archeological find is as important as the morphological characters that currently define each object. Chemical analyses have the potential to reveal much more than simply morpho-species data, but the endogeneity of the material being analyzed is crucial to interpretation. Indeed, the precise elemental inventory of a discrete biological structure may yield potentially crucial phylogenetic information that could refine conclusions beyond a purely morphological approach. Therefore, the collection, storage, and curatorial history of an object are vital to understanding anomalous chemistry that might cause confusion or produce dubious interpretations. The long-term anthropogenic storage of biological and chemical compounds is subject to the same chemical and physical factors that control the preservation of paleontological and archeological material. Fossil and archeological records can reveal the precise chemical alteration pathways that are followed for various materials within a

range of environments. This information may provide answers about long-term processes that are beyond the reach of laboratory experimentation due to time and space constraints. Indeed, paleontological specimens can be considered as relatively well defined long-term geochemical experiments; therefore, such exceptionally preserved fossils may be thought of as the only biogeochemical degradation experiments that have actually run for longer than the 10^5- to 10^6-year periods that are required for safety cases concerning radioactive waste repositories. Therefore, the fields that may directly benefit from such work include materials science, hazardous and radioactive waste disposal, bioengineering, pharmaceutical preservation, and environmental chemistry.

1.2. Challenges and Problems

We have identified five major problem areas that are encountered during the analysis of rare and ancient archeological and paleontological specimens. Each is discussed below.

1.2.1. Degradation and breakdown. Perhaps the most important challenge posed by analyses of ancient material stems from the inevitable degradation of specimens through geologic time. For the organic fraction of a specimen, such degradation can lead to almost complete destruction or alteration of the material of interest (4). In addition, the inorganic materials present may also be significantly altered (1). The familiar chemical processes include racemization, hydrolysis, oxidation, dissolution, dehydration and other volatile loss, and microbial reprocessing (1, 2). Physical processes contribute to this complex set of chemical reactions and may involve crushing due to overburden addition; disarticulation prior to burial; reworking and deposition into "new" environments compared with the original burial matrix; bioturbation by invertebrates; bacterially mediated alteration of the object, matrix, and cements; exposure to high heat; and shearing or fracturing through differential movement via geological activity. Finally, manmade pollution can accelerate or enhance degradation and breakdown, which is often even more problematic for comparatively younger archaeological and cultural artifacts.

1.2.2. Loss through transport. Typically, a fossil or a human artifact represents a chemically distinct portion of a larger system. Certain components are present in higher concentrations within the object of interest than in its surroundings, so the general tendency is for mass to be transferred from the object to the embedding matrix as concentration gradients in the vicinity decrease. Thus, objects such as bone tend to lose part of their calcium (Ca) and phosphorus (P) inventory over time, and ratios of Ca to P can be used as indicators of relative age in some circumstances. Likewise, the organic compounds present may diffuse away, forming a diffuse halo around the object. The cadaver decay islands that are immediately present after death, as a function of bacterial breakdown releasing decay products into surround matrix, can leave a permanent halo as bacterially mediated cements are deposited or existing cements altered (1, 16). Such loss of material may be rapid soon after an object is deposited, and mass-transfer rates may strongly depend on changing environmental conditions, such as ambient humidity, pH, redox potential, the moisture content of the matrix, and temperature. In the case of certain biological tissues, the original chemistry may be either inferred through comparison with existing objects or reasonably estimated through consideration of similar tissues in extant related organisms if the fossil species is extinct. Extant phylogenetic bracketing (EPB) (18) can be used to predict the structure, chemistry, and properties of biological structures possessed by, for example, nonavian dinosaurs (16). Mammal claws are composed of (helical) α-keratins, but bird and reptile claws are composed of (pleated-sheet) β-keratins (e.g., Reference 19). Given that dinosaurs fall within the EPB of birds and crocodilians, EPB suggests that the claws of dinosaurs were probably composed of β-keratins (20). However,

in many cases the preferential removal of one or more components may be difficult to resolve and may require careful analysis of the surrounding materials, as well as the object itself, to discern loss through transport.

1.2.3. Overprinting or mass addition. Acting in opposition to mass loss are processes that may add nonoriginal material to an object. Here, geochemical fluids are a key vector for transporting chemicals through porous media or through fractures; when the slightly different chemistry maintained in the vicinity of the object is encountered, these fluids may deposit material through precipitation or by adsorption of organic or inorganic species onto endogenous solids. This process of fossilization defines the final composition of a fossil (16). Again, this process can be difficult to account for; a characterization of mineral precipitates on bedding planes, along fractures, and within the fossil itself can aid in deciphering this process. Indeed, fluids may add components even prior to burial; therefore, this is a crucial issue in paleontology. Similar processes of transfer from containers, handling, storage, or surroundings may affect archeological objects.

1.2.4. Contamination during sampling and analysis. Along with the problem of natural processes adding extraneous material to an object, contamination may also occur through the excavation, preparation, conservation, sampling, curation and storage, and analysis processes (3). Some such contamination may be deliberate, as when curators and conservators use consolidants to conserve an object or use glue to affix labels to specimens while unaware of the high levels of trace metals found in many adhesives. Modern analytical methods can resolve traces of contamination that Victorian-era curators would probably never have thought possible. We are developing protocols based on organic chemistry methodologies to ensure that our paleontological samples are kept as pristine as possible (2, 4); however, our sampling and handling methods are by no means universally applied, and inadvertent human contamination will continue to pose a problem in the analysis of specimens handled by untrained personnel (3). Indeed, we can resolve the fingerprints of those who have handled many of the specimens we analyze (3).

1.2.5. Damage from analysis. Many analytical tools destroy at least part of the object under investigation. In some cases, for example, carbon-14 dating and neutron activation, a small sample of the object can be extracted, but this is not always possible, particularly with valuable specimens. X-ray techniques are generally nondestructive at sufficiently low doses. However, X-rays may cause some damage by, for instance, drying out the parchment of an ancient manuscript or photoreducing the chemical environment of a transition metal in a valuable fossil. Therefore, damage studies must be performed in some cases, and the efficiency of the measurement needs to be optimized to allow for the smallest necessary dose. We discuss some of the mitigations of potential damage from X-rays in the following sections.

2. TRADITIONAL METHODS

Since the electron microprobe became commercially available in the 1950s, it has become the standard technique for the analysis of geological materials. Advances in electron optics have made it possible to image objects at micrometer resolution through the use of electron microscopy; later, the refinement of pressure-limiting apertures (PLAs) led to enormous possibilities for imaging and analysis without the need for coating the surface or subjecting fragile samples to high vacuum. Electron-beam techniques have thus served as standard methods for both chemical and ultrastructural analysis. Recent work in paleontology has used this imaging capability to study the morphology of numerous delicate structures preserved in fossils, including those interpreted as melanosomes (21, 22), epidermal cells (1), muscle cells (23), and the cartilage structure within

the interlacunar matrix of primitive fish (24). The chief limitation on electron-beam techniques is that, even for commercial instruments equipped with a PLA, the sample must fit into an analytical chamber, so the sample size is limited to ~20 cm or smaller. The flux of electrons is relatively small, so mapping the distributions of trace elements can be time consuming, which is compounded by the fairly high bremsstrahlung that is generated in the sample by the beam. Ion-beam techniques, in particular proton probe methods, are also widely used for the analysis of mineralogical specimens. The proton probe has two advantages relative to the electron probe. First, due to the high mass of the proton relative to that of the electron, the proton beam does not spread as much as the electron beam, so zoning studies can be completed with higher spatial resolution. Second, much lower intensity (two to three orders of magnitude) bremsstrahlung radiation is created when protons are used to excite characteristic X-rays; therefore, this technique can resolve compositional features at the parts-per-million level, whereas the electron probe struggles at concentrations below 100 ppm.

Synchrotron-based methods, especially XRF methods, are undergoing development at many locations because the extremely high flux of photons available at the current generation of synchrotrons means that quantification is possible even with ultradilute samples. High flux also means that ever smaller pinholes may be used, so spatial resolution can become better and better; currently, a resolution of 100 nm is possible. Perhaps most importantly, synchrotron-based XRF can conveniently be augmented with microdiffraction and micro-EXAFS (extended X-ray absorption fine-structure) analysis, which adds several key pieces of information. The next section discusses synchrotron methodology in detail.

3. SYNCHROTRON METHODS

SR was originally a parasitic by-product of high-energy physics experiments, but it started to be used for various X-ray studies in the 1970s (25). Over the past 30 years, this technique has evolved into a powerful research tool in many dedicated facilities around the world that serve tens of thousands of scientists per year. The spectrum of SR ranges from the low-IR regime up to the hard-X-ray regime. Along with some applications in the IR regime, most scientists use the vacuum UV and X-ray spectra of SR. SR-based X-ray beams have several crucial advantages compared with conventional X-ray tubes. These include the easy tuning of the X-ray energy, the polarization of the X-rays, and most importantly, the immense brightness. Less often exploited is another quality of SR, namely the fact that SR pulses are very short (of order tens of picoseconds) and can be used to study fast time-dependent phenomena. Insertion devices at the powerful third-generation SR facilities can produce very intense collimated beams with a brightness that is more than 10 orders of magnitude greater than that produced by conventional X-ray tubes. As such, not only is SR a very powerful tool with which to perform X-ray diffraction and X-ray spectroscopy experiments, but it can be used for imaging work, sometimes in combination with these techniques. Although all the techniques described below take advantage of one or more of the unique properties of SR, this review focuses on the recently developed technique described in the next section.

3.1. Synchrotron Rapid Scanning X-Ray Fluorescence

A two-dimensional elemental map of an object of interest can be obtained by detecting the XRF signals at each spot when a focused X-ray beam is raster scanned across the object. The spatial resolution of the elemental map (the XRF image) is determined by the footprint of the X-ray beam that strikes the object, and the XRF image is reconstructed from all these individual points (pixels). The required spatial resolution and the size of the object determine the number of pixels needed for an XRF image. With new X-ray optics, ever smaller X-ray beams are now available

at modern SR facilities. Scientists have recently developed X-ray microscopes with resolutions well below the micrometer range—as good as ~10 nm (26, 27; also see the next section). Such microscopes are, of course, limited to imaging extremely small areas, but there is also a need to obtain XRF images of the entire area of larger objects such as fossils, manuscripts, or paintings. The following example illustrates the challenges related to such work.

An object of the size of an *Archaeopteryx* fossil (~40 cm × 50 cm) requires 2×10^7 pixels, that is, 2×10^7 individual XRF measurements when imaged with a pixel edge length of 100 μm. To obtain such an image on a practical timescale (on the order of several hours), the readout time to obtain the XRF spectrum at each pixel must be very short (on the order of milliseconds). To acquire sufficient XRF signal statistics during such short exposure times, one needs a very intense, fine, and collimated X-ray beam, which is available only at an SR source. Furthermore, to avoid any additional dead times, the readout has to be done "on the fly," that is, while the object is being scanned. Such a system has been developed at the Stanford Synchrotron Radiation Lightsource (SSRL) at SLAC National Accelerator Laboratory and is the basis of the synchrotron rapid scanning XRF (SRS-XRF) imaging technique described herein. Originally developed for the imaging of the Archimedes Palimpsest (5–8), the setup at SSRL has been used to image and study various samples, including manuscripts, slices of brain for medical research, and fossils (2, 3, 4, 9, 10, 28–31). This system has evolved into a very powerful setup with a scanning rate as fast as 3 ms per pixel, which allows a 10-megapixel digital image to be produced in less than 10 h. Other SR-based XRF studies of, for example, paintings, are currently being pursued at various SR facilities, most notably the European Synchrotron Radiation Facility in Grenoble, France (11–13). We briefly describe the concept of SRS-XRF here; a more detailed description of the SSRL setup is given elsewhere (8).

Figures 1 and **2** present the physical arrangement of the SRS-XRF scanning setup at SSRL, where most of the images shown were taken. Located in the straight section of the 3-GeV SPEAR3 storage ring is the 54-pole wiggler (1 T) that feeds beam line 6–2. The X-ray beam is collimated with a total-reflection mirror, passed through a Si(111) monochromator, and then doubly focused (in the horizontal and vertical directions) with a second total-reflection mirror onto a collimator slit, which is followed by a spherical pinhole aperture prior to illumination of the sample (**Figure 1**). The combination of the collimator slit and the pinhole size and the distance between them define the divergence of the pencil-like beam. Ideally, the sample is placed very close to the pinhole to minimize any effects of such beam divergence.

Often the XRF detector is placed so as to optimize the geometry for the detection of fluoresced X-rays and to minimize the amount of scattered radiation entering the detector windows

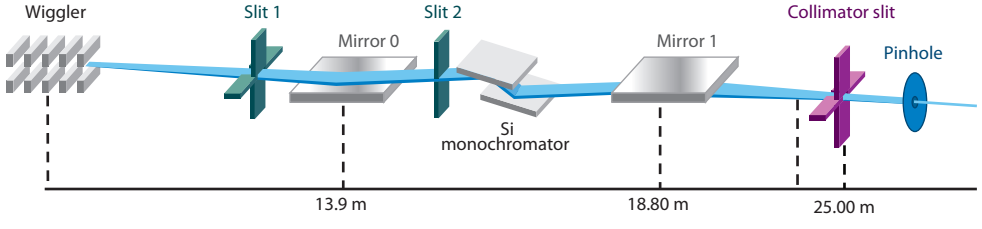

Figure 1

Schematic outline of Stanford Synchrotron Radiation Lightsource beam line 6–2. X-rays created in the 54-pole wiggler are collimated by a total-reflection mirror onto a Si(111) monochromator and focused by a doubly focusing total-reflection mirror onto a collimator slit. The tantalum pinhole slit is aligned to produce a highly collimated beam for X-ray fluorescence imaging.

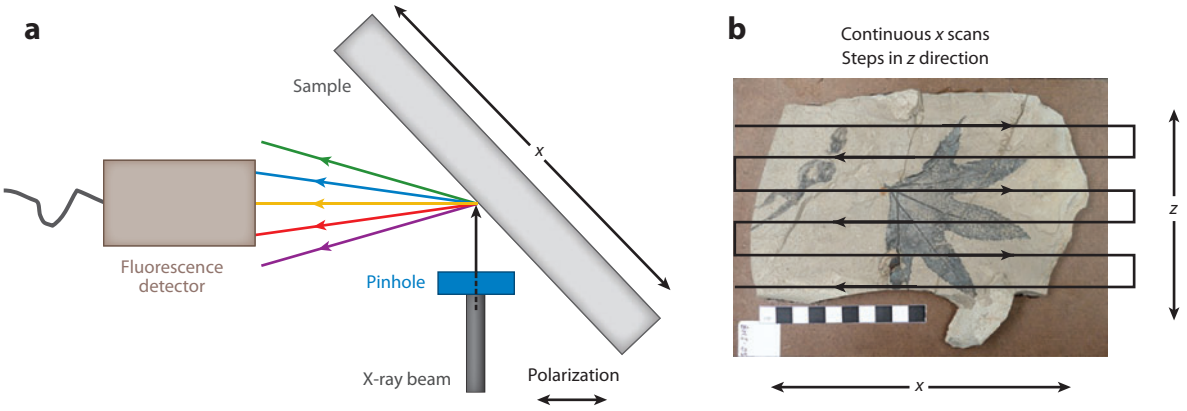

Figure 2

(*a*) Top view of the schematics of the X-ray fluorescence (XRF) imaging setup. The XRF detector is placed perpendicular to the incident beam. The XRF, schematically shown with different colors, is emitted in all directions, and some fraction of it is captured by the detector. (*b*) Schematics of synchrotron rapid scanning XRF imaging. Horizontal (*x*) scans are performed continuously, and at the end a vertical (*z*) step is performed.

(**Figure 2**). SR radiation is polarized horizontally; therefore, the XRF detector is placed at an angle parallel to the polarization direction and 90° horizontally with respect to the beam direction (**Figure 2**). This angle corresponds to the X-ray Brewster angle, where the scattering is minimal and the detection of fluoresced X-rays is optimized. Ion chambers are used to monitor the flux of the incident X-rays. Note that for the imaging of parchment leaves (which are largely transparent to X-rays), a second XRF detector is placed behind the sample at 90° to the right, which allows for discrimination of the writing on both sides of the parchment (7). Samples are mounted on a motorized stage and then raster scanned relative to the beam. Scans are rapid and continuous in the *x* direction; the detector electronics are precisely timed in synchronization with the stage control, such that X-ray detection coincides with the speed of the stage motor. Each pixel recorded therefore represents an area on the sample that is approximately equal to the size of the pinhole aperture. At the end of each raster line, the stage is stepped in the *z* direction, and a new line is recorded. Data were recorded on the fly in both horizontal directions at a rate typically corresponding to ~3 ms per readout. The beam intensity was monitored with a helium (He)-filled ion chamber upstream of the pinhole. During scanning, small drifts of the beam with respect to the pinhole were periodically corrected.

The SRS-XRF method relies on several critical advantages that SR has over X-ray tubes. The much larger brightness allows for a small, intense, and collimated beam with a long focal length, which ensures that an object with an irregular surface, such as an uneven parchment or fossil, is in focus throughout scanning. Furthermore, SR is polarized, monochromatic, and energy tunable, which helps minimize unwanted scattering background and unwanted XRF from elements that are not of interest. Consequently, the rapid scanning technology allows the fluoresced signal to be mapped quickly even for elements present in trace quantities. Beam line 6–2 can operate in an energy range from 2.4 to 17 keV, and for each study the excitation energy is optimized. For example, for light-element XRF images [chlorine (Cl), sulfur (S), P, and potassium (K)] of the fossils, an excitation energy of 3.15 keV was chosen; for the heavy-element images [Ca, manganese, iron (Fe), nickel, copper (Cu), zinc (Zn), selenium, barium, and lead], excitation energies ranging from 9 to 13.5 keV were chosen. Flux at the sample surface varied between approximately 10^{10} and 10^{11} photons s^{-1}, depending on the specific analytical conditions. The beam size was set by

100-μm-thick tantalum pinholes with a 50- or 100-μm-diameter aperture, depending on the required resolution. Samples were mounted close to the pinhole at either 45° (high incident energies; see **Figure 2**) or 67° (low incident energies) relative to the incident beam. A photon-counting single-element silicon drift detector (Vortex®, SII NanoTechnology USA, Inc.), combined with Gaussian shaping amplifiers (Canberra Industries, Inc.) employing 0.125-μs shaping times plus single-channel analyzers, was used to detect the XRF signals. For each chemical element, the electronic windows were set to capture the fluorescent photons from the Kα or Lα emission lines.

For scans in the excitation energy range between 9 and 13.5 keV, the detector was placed at a 90° angle relative to the beam to minimize the unwanted scattering signal (see above discussion). For scans at 3.15 keV, the detector was placed normal to the sample surface in order to minimize attenuation of the XRF signal. Note that for these low-energy X-rays, the scattering background signal is much weaker; therefore, the Brewster angle geometry is not required. All the fossil and extant samples were held within a purpose-built sample chamber that was carefully mounted on a computerized *x-y-z* translational stage. For the light-element XRF imaging, an X-ray-transparent ~30-μm-thick polyethylene film was placed on the sample chamber, and the chamber was purged of air with He. For the imaging of the *Archaeopteryx* fossil, which has a limestone matrix, we placed a 50.8-μm-thick aluminum (Al) foil in front of the detector to reduce the very large Ca signal produced when studying the heavier elements. Both the air absorption and the Al foil reduced the Ca Kα fluorescence by a factor of 500, whereas the 3d transition metal signals were reduced only by 20% to 80%.

3.2. Micro-X-Ray Fluorescence

In certain circumstances, it is preferable to produce elemental distribution maps at as high a resolution as possible to compare chemistry with ultrastructural details. Microfocused beam technology can be used for this purpose. Much effort has been devoted to the use of microfocusing technology to analyze environmental samples in which the sediments or soils are extremely heterogeneous and the contaminant levels are low. An early application of this technique in the field of paleontology was in determining the zoning patterns of Cu in fossilized bird feathers (4). The structural details of these feathers had been completely reacted away, but by mapping the Cu distribution and showing that the trace metal was distributed in patches ~2 μm in size, the authors of this study showed that the size of the chemical deposits were consistent with the hypothesis that the Cu was the residue from the breakdown of eumelanin pigment synthesized within melanosomes, organelles whose size typically ranges between 0.5 and 3 μm.

3.3. X-Ray Absorption Spectroscopy

X-ray absorption spectroscopy has been applied to geological samples for more than 30 years. It was initially used in the study of noncrystalline phases (silicate glasses) because such solids are not amenable to structural study by the older technique of X-ray diffraction. However, it quickly became clear that because X-ray absorption spectroscopy is element specific, it can be used to obtain critical local coordination information for trace components held within both amorphous and crystalline structures.

X-ray absorption spectroscopy exploits the fact that the synchrotron ring essentially produces a white X-ray beam tangential to the direction of travel of the electrons in the ring. By using a monochromator to select a single X-ray energy from this white beam, one can analyze a sample by scanning the incident beam through the critical excitation energy pertinent to the ejection of a photoelectron. The classic experimental geometry involves placing an ion chamber upstream of a thin sample to monitor the incident beam intensity, then placing a second ion chamber downstream of the sample to monitor the transmitted intensity. By scanning through the critical

energy, slight oscillations in the absorption coefficient become apparent; these oscillations include both XANES (X-ray absorption near-edge structure; from slightly below up to approximately 50 eV above the edge) and EXAFS (up to approximately 1,000 eV above the edge). Once the energy of the incident beam exceeds the critical energy for photoelectron ejection, the outgoing electron is considered a wave that can be scattered by the surrounding atoms. Backscattering causes interference with the outgoing wave; this interference causes oscillations in the absorption coefficient. The frequency of EXAFS oscillations depends on the distances to the surrounding backscattering atoms. The amplitude of these oscillations depends on the type and number of the surrounding atoms. Via EXAFS, the distances can be precisely resolved down to 0.01 Å or better. Analyses of standard compounds where the coordination environment is already known can rapidly speed up the interpretation of EXAFS data. For elements that display more than one oxidation state, the XANES spectrum can be used to determine the oxidation-state speciation of a complicated mixture of valencies. More detailed reviews of EXAFS analysis can be found in References 32 and 33.

3.4. Synchrotron Fourier Transform IR Spectroscopy

Cotte et al. (14) recently reviewed advances in the use of Fourier transform IR spectroscopy (FTIR) to characterize archeological specimens. More recently, Reiche et al. (15) used synchrotron FTIR mapping and spectroscopic analysis to resolve the chemistry and structure of a 5,000-year-old mammalian bone. This study sought to use the relatively high spatial resolution of the synchrotron IR beam to resolve the distribution of chemical functional groups with the fine structure of bone; the authors succeeded in mapping at the osteon scale (20 to 70 μm). Furthermore, the authors analyzed details of the antisymmetric stretch of the phosphate groups on the basis of the fact that the intensity ratio of the peak at 1,030 cm^{-1}, relative to that at 1,020 cm^{-1}, can indicate hydroxyapatite crystallinity. For modern samples, this ratio tends to be approximately equal to one; with aging, crystallinity tends to improve, so the value of this ratio increases. A high value of this ratio—as for the specimen analyzed in this study, which had a 1,030:1,020 ratio, equal to 1.32—indicates that significant alteration of the bone had occurred.

3.5. Tomography

In closely related research, computational modeling of locomotion has taken advantage of computed tomography (CT) scanning to improve estimates of muscle mass and thereby produce more accurate results. Synchrotron-based CT scanning can provide submicron resolution and has been used to provide three-dimensional images of feathers preserved in amber from the Cretaceous period (34). The results indicated that the feathers may have come from either primitive birds or nonavian dinosaurs. In the future, results of tomography studies will be used to improve computational models of dinosaur locomotion and to constrain the evolution of locomotor pathways for the dinosauria (35).

4. CASE STUDIES

4.1. Synchrotron Rapid Scanning X-Ray Fluorescence Imaging of the Qur'ān Palimpsest

Palimpsests are manuscripts on which, in an ancient form of recycling, the original writings were partly erased and overwritten with newer text. Palimpsests were common throughout several

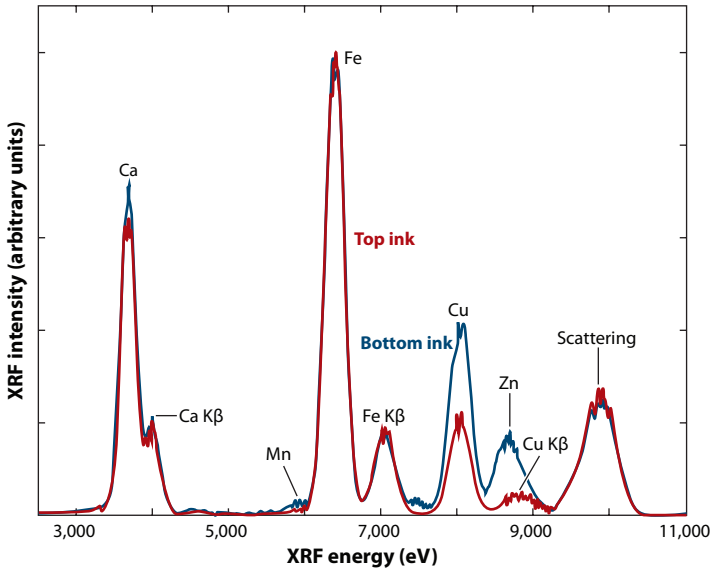

Figure 3

X-ray fluorescence (XRF) spectra from the two inks of the Qur'ān palimpsest. All lines are Kα unless indicated otherwise. Note that spectra have been normalized to yield the same Fe Kα signals.

centuries when parchment was used. In the case of the Archimedes Palimpsest, parchment leaves from a tenth-century copy of works by Archimedes were reused in a prayer book that was completed by Johannes Myronas on April 14, 1229. Although the chemical compositions of the two iron-gall inks are very similar, SRS-XRF imaging was successful in distinguishing the underlying writing because the orientations of the two texts differ by 90°, allowing them to be readily distinguished (6, 7, 8). Furthermore, inks on the front and back sides of this palimpsest were distinguished through the simultaneous use of two XRF detectors, one in the front and one in the back (7). Other palimpsests were overwritten in the same orientation as the original text. In such cases, it is more difficult to discern the two texts. **Figure 3** shows the XRF spectra of the two inks of a palimpsest that is possibly the oldest known source of the Qur'ān. The parchment was radiocarbon dated to the time of the prophet Muhammad (9).

The true energy widths of XRF lines are only a few electron volts, but the measured widths, as shown in **Figure 3**, are broadened by the energy resolution of the detector system. However, this resolution is sufficient to discern different fluorescence lines. In fact, these two XRF spectra revealed a striking difference in the composition of the two inks: In the younger, top ink, the Cu signal is strongly reduced and the Zn signal is essentially absent. In **Figure 4**, the visible image is compared with Fe and Zn XRF maps. As expected from the XRF spectra, in the Fe map both inks are imaged, but the Zn map shows predominantly the older, overwritten text.

These XRF images have enabled a detailed study of this leaf of the Qur'ān palimpsest, bringing to light features of the text that were not visible otherwise (9). Whereas the upper layer of writing is a standard Qur'ān, the underlying (older) layer of writing does not belong to the standard textual tradition. Through a detailed textual analysis, Sadeghi & Bergmann (9) argued that the lower text of the palimpsest, the standard Qur'ān, and the other known versions of the Qur'ān (belonging to associates of the Prophet) form parallel textual traditions. Comparison can thus illuminate the state of the Qur'ānic text prior to the branching off of these various traditions, which sheds light on the progenitor of all of them, the Qur'ānic prototype.

Figure 4

(*a*) Visible-light images of both sides of a single leaf of the Qur'ān palimpsest. (*b*) The enlarged area corresponds to the red box in panel *a*. (*c*,*d*) X-ray fluorescence images of (*c*) Fe and (*d*) Zn.

4.2. Cherubini and the Restoration of Lost Art

As a second example of how SRS-XRF mapping can reveal information that has apparently been lost, we consider the manuscript of an opera by the Italian composer Luigi Cherubini from the late eighteenth century. The original script of the opera *Médée* was overpainted at some point in its history, completely obscuring the aria "Du trouble affreux qui me dévore" from the third act. Preliminary chemical analysis revealed that several different trace metals were present within the ink Cherubini used to write his score, so full SRS-XRF scans of the overpainted pages were performed.

Figure 5 shows overpainted pages in which large sections are completely obscured. **Figure 6** illustrates the scanning setup used at SSRL to analyze the Cherubini score. The rear emission volume was drawn smaller, given that paper absorbs some of the transmitted incident beam, and therefore, the number of characteristic photons produced from the reverse side is slightly less than in the front. The detectors were mounted to both front and back to register the emitted intensities as the manuscript was scanned in the beam.

Figure 7 shows the spectrum of X-rays emitted from the manuscript and highlights the characteristic energies of K, Fe, and Zn. **Figure 8*a*** presents a single-element map of Zn, revealing that the ink used to print the staff lines on the manuscript paper was singularly rich in this trace

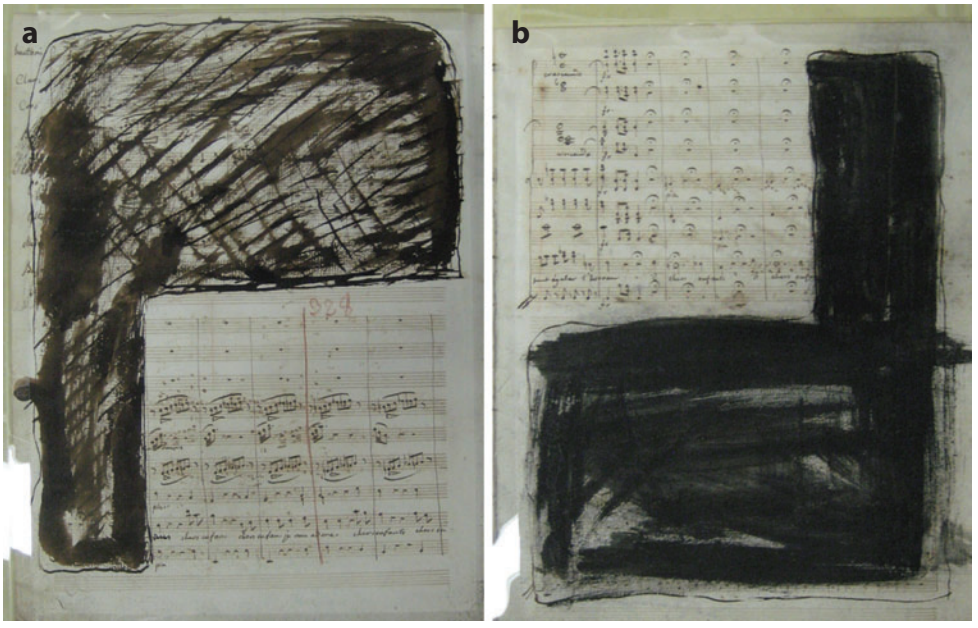

Figure 5

Optical photographs of (*a*) the front and (*b*) the back of the overpainted Cherubini manuscript.

metal but that the ink used to write the musical score did not contain appreciable quantities of Zn. However, **Figure 8*b***, a single-element map of Fe, clearly shows that Cherubini used an ink that contained high concentrations of Fe, presumably iron-gall ink, which was prepared by adding ferrous sulfate to a tannic acid solution. This ink was standard in Europe during the composer's lifetime. However, the X-ray emission signal from Fe is at a high energy of 6.4 keV. At this energy, the manuscript paper absorbs very few of the emitted X-rays, so it is difficult to distinguish writing on the face of the paper from ink on the reverse side: The two signals become confused. However, there is also a significant amount of K in the composer's ink, and the emission energy of K is much lower at 3.3 keV. In this case, the paper absorbs enough of the emitted radiation that text on both the front and the back can be distinguished, as shown in **Figure 8*c*,*d***, which compares the K distribution mapped by an X-ray detector facing the front of the manuscript page with the distribution mapped by a second detector facing the back. These images are blurry, but the front and back signals are different. By using the K maps to differentiate front from back and then combining the Fe maps with the deconvolved K signals to enhance the clarity of the writing, one can decode notation on both the front and the back (**Figure 9**). Fortunately, the ink used to overpaint the musical score was apparently not iron-gall ink but rather India ink or carbon black. India ink and carbon black have low quantities of trace metals, so the overpaint does not significantly interfere with X-ray mapping.

4.3. Archaeopteryx, Dinosaurs, and Green River Reptiles Give Insights into Soft-Tissue Preservation

Perhaps one of the most important fossils ever discovered, *Archaeopteryx* provided pivotal evidence for Darwin's theory of evolution by natural selection just a few years after the publication of

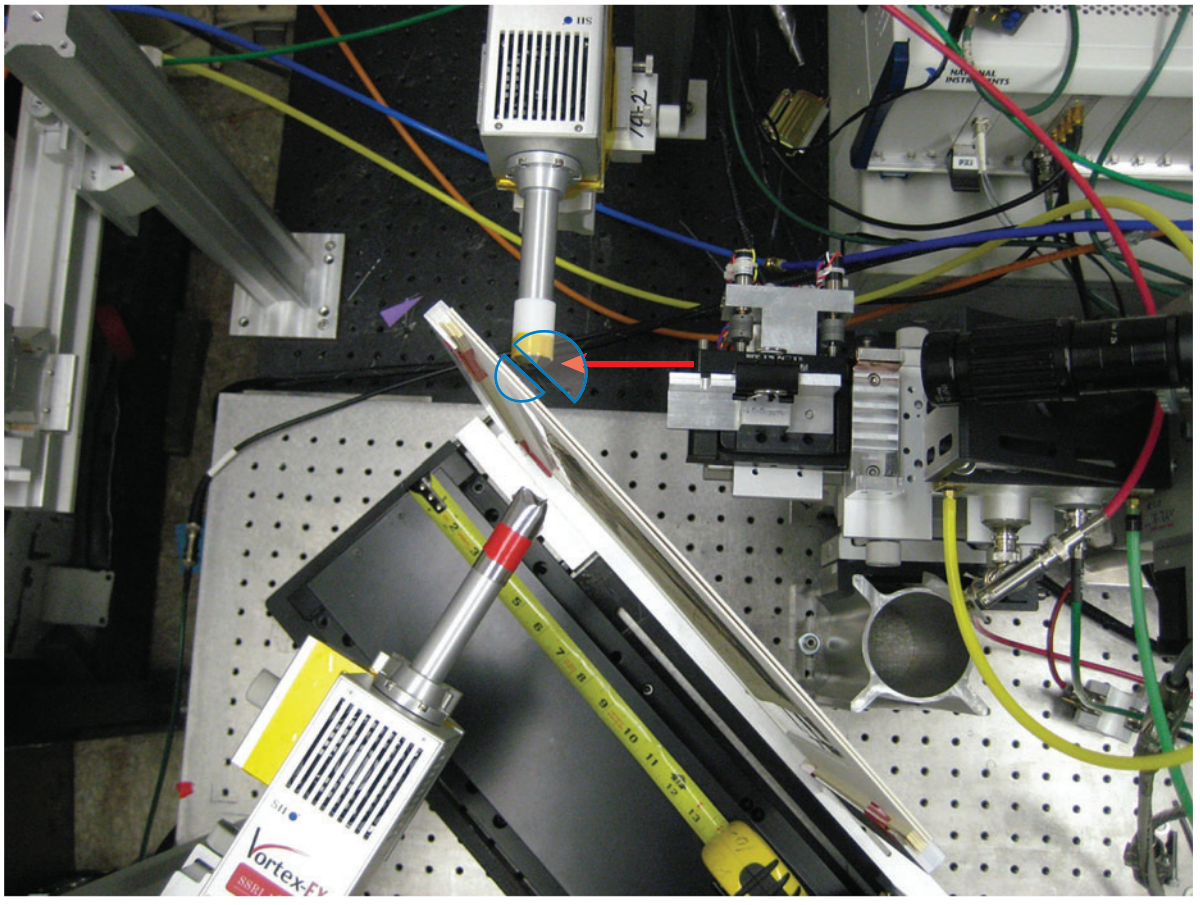

Figure 6

Synchrotron rapid scanning X-ray fluorescence setup used for the Cherubini manuscript. The incident X-ray beam is indicated by the red arrow; the incident photons traveled in the direction of the arrow. The Cherubini manuscript was mounted vertically, and the X-ray emissions are indicated by the blue semicircles in the front and back of the manuscript.

On the Origin of Species (36). Found in a limestone quarry in southern Bavaria, *Archaeopteryx* provided strong evidence for the now universally accepted evolutionary link between dinosaurs and birds. The fossil captures a very rare transitional species: *Archaeopteryx* had wings and feathers like a bird but retained a long bony tail, teeth, and claws on its forelimbs like a reptile (37). Indeed, the tremendous detail in the feathers of several preserved *Archaeopteryx* specimens provided the first evidence for when and how birds evolved. The delicate detail of these feathers had always been assumed to be due to impressions that the feathers had left behind in the very soft, fine-grained carbonate sediment in which they were deposited. No trace of the original soft-tissue chemistry was believed to remain. However, research into bone and soft-tissue preservation took several important steps forward during the past decade. We review this progress below, then return to how modern analytical methods revealed new, unexpected chemical information about *Archaeopteryx*.

Techniques developed within the biological sciences have recently been adapted for use in the study of fossil remains (38). Although findings have been encouraging, some results with bone

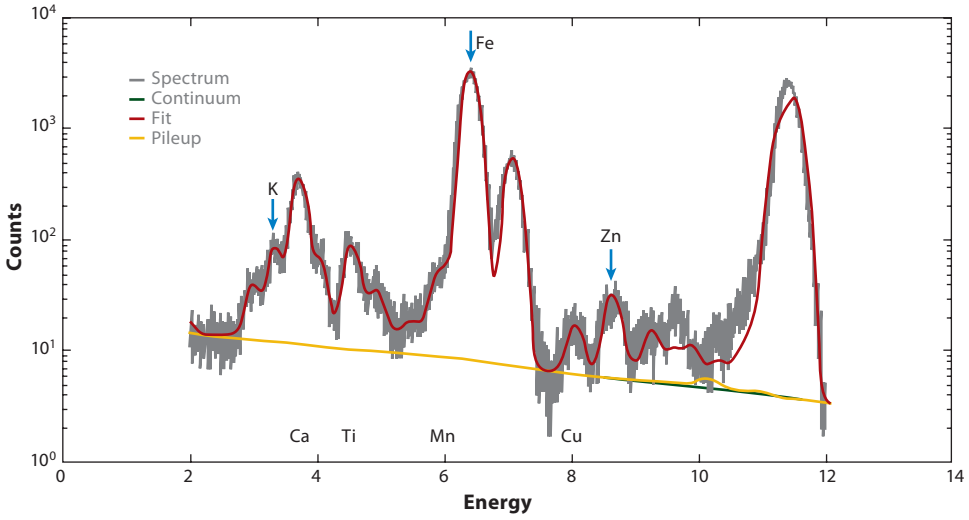

Figure 7

Energy-dispersive X-ray fluorescence spectrum from the Cherubini manuscript. The elements associated with the chemistry of the composer's ink (K and Fe) and the printed staff lines (Zn) are indicated with blue arrows. By selecting these characteristic energies and mapping their intensity distributions on the page, one can detect the staff lines and the composer's notations through the overpaint.

collagen and other organic material from extremely old paleontological specimens (39) are still under scientific debate (40). Trace-element mass spectrometric analysis with laser ablation has also provided important insights into how fossil material reacts with the embedding matrix over geological time (41).

In a recent study focused on soft tissue, examination of the skin envelope of an exceptionally well preserved hadrosaurian dinosaur (MRF-03) allowed traces of the original skin chemistry to be resolved through the use of a range of modern analytical techniques (1). The skin samples from MRF-03 (taken from the ventral surface at the base of the tail) indicated that the skin was ~2.5–3.5 mm thick, and the preserved internal structure was visible through scanning electron microscopy (SEM) (1). Compositional data were also recovered through energy-dispersive X-ray (EDX) analysis, but the results were too crude to provide information about the spatial distribution of the trace-element inventory of the skin. However, the SEM data indicated that the organic compounds were restricted to within the skin envelope. The specimen was then analyzed by both IR and mass spectroscopic techniques to further resolve the presence and the identity of organic compounds.

FTIR was used to map the presence of IR-active organic functional groups in skin, hoof, and tendon samples from MRF-03. The position and appearance of the FTIR bands of the amide I and II groups present within the skin regions of MRF-03 were similar to what was measured in extant β-keratin samples taken from bird and reptile tissues (1), which showed that the residue from the hadrosaur skin is comparable to analogous biomaterials and is thus compositionally constrained by the EPB (1, 18). The presence of the amide groups signified that intact proteins or their breakdown products may have survived in MRF-03.

Pyrolysis gas chromatography mass spectrometry showed that the skin's organic inventory was distinct from the embedding silicate sediments. Amino acid analysis confirmed those results, although not enough material was present for a full proteomics analysis. However, one of the

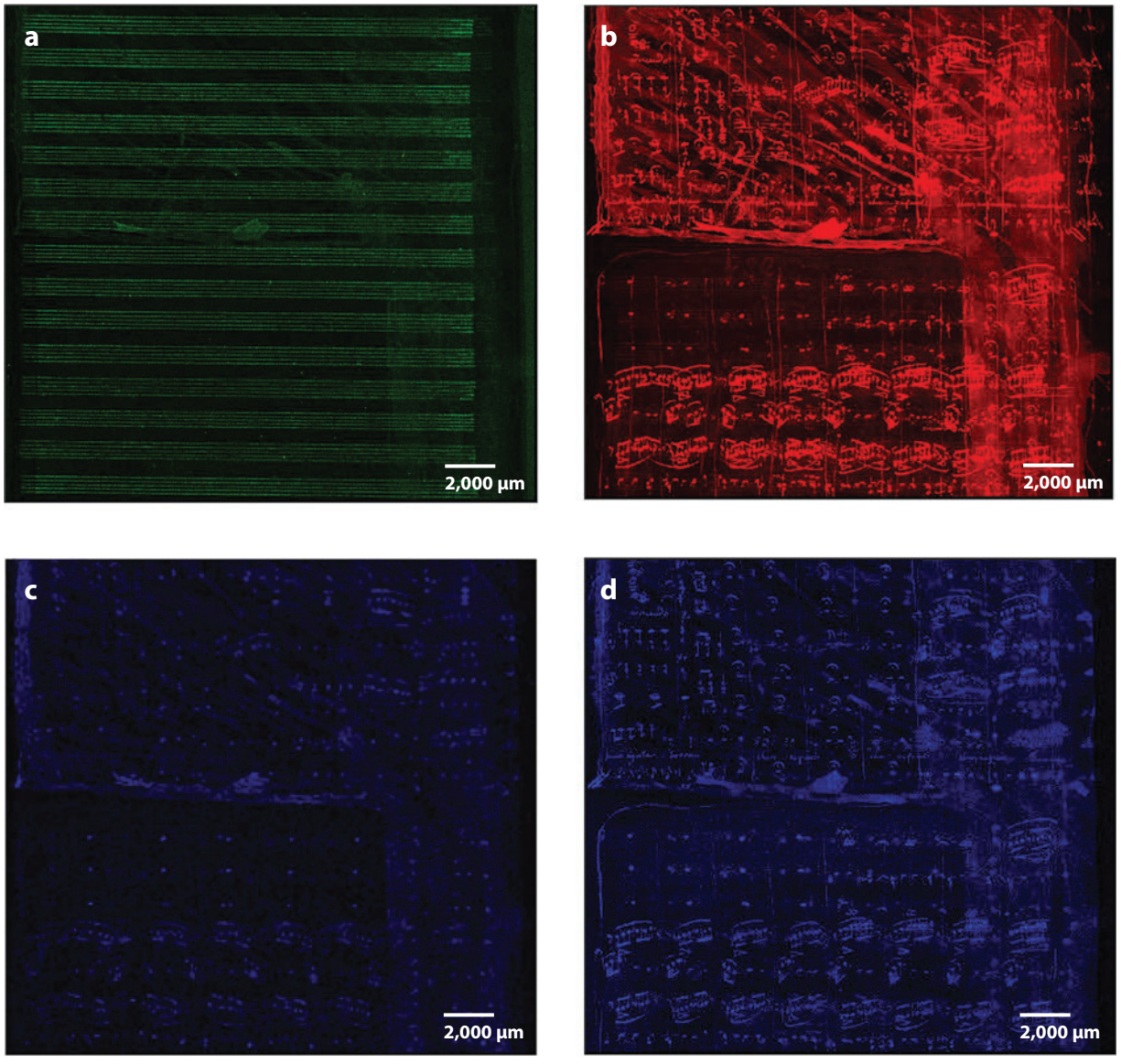

Figure 8

(*a*) Synchrotron rapid scanning X-ray fluorescence (SRS-XRF) map of Zn, showing that the staff lines were printed with ink that contained appreciable quantities of that metal. (*b*) An Fe map of the same region, showing that the composer's ink was high in Fe. Close examination reveals that notation from both the front and the back of the page are superimposed due to the transmission of the relatively high energy Fe X-rays through the paper. A K SRS-XRF map of (*c*) the front and (*d*) the back of the same region in panels *a* and *b*. K is also contained within the iron-gall ink, but attenuation of the K fluorescence by paper is much greater, resulting in a reduction in superposition of the notation.

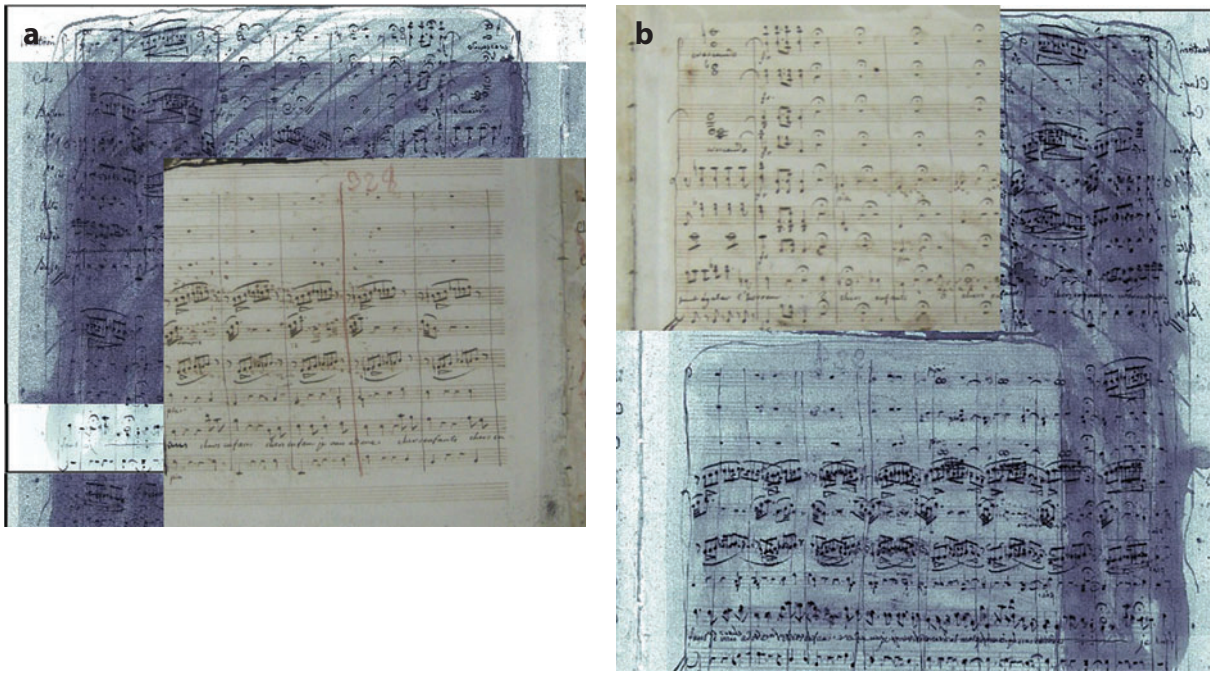

Figure 9

By setting a threshold on the K maps and then correlating K with Fe, one may resolve the notations on the front and the back. (*a*) Part of the front of a page, in which the exposed section of text has been matched up with that revealed by synchrotron rapid scanning X-ray fluorescence. (*b*) The back of the page.

most promising results was that, through the use of a modern FTIR instrument to image the specimen, the amide I and II absorption bands were mapped to show that organic residue coated sedimentary grains from within the skin envelope of the dinosaur, and the detailed spectroscopy of these bands strongly resembled that of β-keratin samples from modern birds and reptiles. These results suggested that assumptions about soft-tissue preservation in other specimens may need to be reassessed. Furthermore, chemical maps of the skin performed with the electron microprobe provided clues about the geochemical pathway that led to the exceptional preservation. Electron microprobe maps of the Ca distribution within the hadrosaur skin envelope essentially provided a map of a secondary precipitate of the mineral calcite, $CaCO_3$ (which, in this case, geologists refer to as a mineral cement), revealing a cell-like structure. This finding was interpreted as reflecting a rapid precipitation event during which original skin cells were either replaced by calcite or coated before they had completely degraded. This structure created an exceptional environment for soft-tissue preservation, which led to the remarkable detail that remains visible in the skin, as well as the persistence of some of the chemical features of the original β-keratin, such as the clear presence of amide functional groups within the skin regions. Taken together, all of these results indicated that the analysis of fossil soft tissue with modern methods could reveal exciting new chemical details about both the original organism and the process of exceptional preservation.

When the use of nondestructive SRS-XRF to analyze large specimens became possible at SSRL, investigators selected several fossil specimens of great scientific importance, especially *Archaeopteryx*, to test whether SRS-XRF could be successfully used to resolve the chemical fossil residue within soft-tissue regions. SRS-XRF was chosen as the primary tool for this research

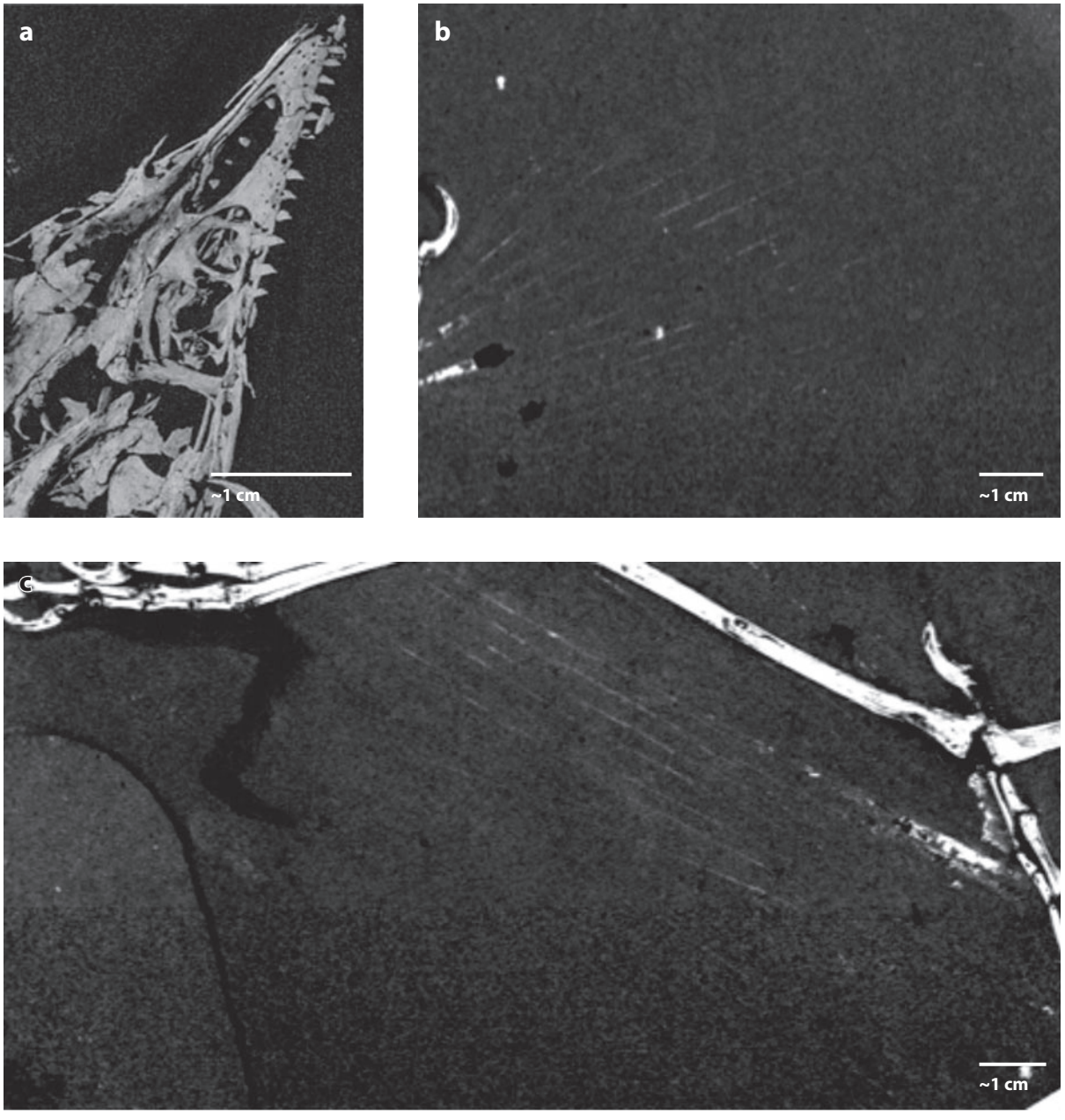

Figure 10

Synchrotron rapid scanning X-ray fluorescence detail maps of P distribution within the Thermopolis *Archaeopteryx*. (*a*) Skull detail that resolves additional teeth obscured by sediment. (*b*,*c*) Feather shafts (rachises) revealed for the first time to be chemical remains of soft tissue, not merely impressions. Adapted from Reference 3.

Figure 11

Zn distribution in the Thermopolis *Archaeopteryx*. Zn levels are only 10 to 50 ppm in the bone, and the background levels in the sediment are as high as 20 ppm, so contrast is low. However, mapping clearly reveals elevated and relatively constant concentrations of this key nutrient within the fossil bones. Adapted from Reference 3.

because trace-element patterns should still be resolvable even when all of the organic material has completely degraded away. Furthermore, correlation of elemental patterns with biological structure could also serve as a critically important scoping tool to pinpoint hot spots or regions of interest for more detailed FTIR imaging or for pinprick destructive sampling.

In the first set of analyses, SRS-XRF mapping of the Thermopolis *Archaeopteryx* specimen produced several clear scientific results (3). Not unexpectedly, the bone matter was easily mapped; indeed, several teeth that are not apparent in visible light become clear when imaged in P (**Figure 10*a***). However, the full chemistry of the bone was revealed by mapping, and quantitative XRF point analyses completed during the scanning runs allowed for scaling of the maps in terms of elemental concentration. Cu and Zn are critically important macronutrients in the diets of captive birds. The point analyses and maps of these two elements in the *Archaeopteryx* bones showed that their concentrations are very similar to those documented for modern bird species, strongly suggesting that the nutrition requirements of *Archaeopteryx* were similar to those of modern birds (**Figure 11**).

Another feature of the P maps may be the most interesting result from this study. **Figure 10** shows a black-and-white map of P within parts of this specimen and reveals that the feathers are clearly not impressions; rather, the feather shafts (rachises) stand out as enriched in P relative

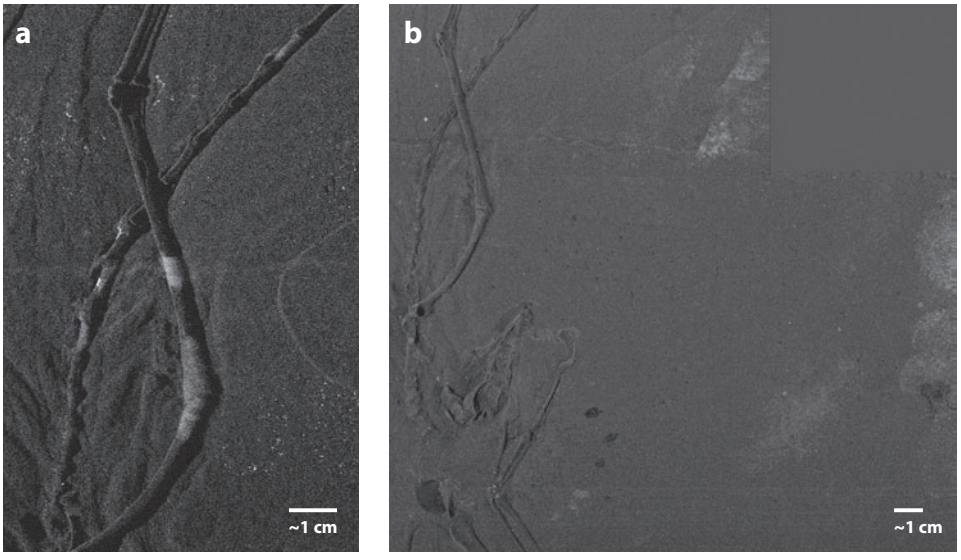

Figure 12

(*a*) Br anomaly indicating areas where artificial fill was added to the fossil. (*b*) Fingerprints at the periphery of the sample revealed through the mapping of Cl. Adapted from Reference 3.

to the sedimentary matrix (**Figure 10*b*,*c***). This patterning is also observed with S. The P and S concentrations within the feathers are lower than in modern bird feathers, so there is no need to invoke the addition of these elements through geochemical processes to explain these patterns. Indeed, given the levels of S and P in the sediment, mass transfer of these two elements should be in a direction away from the fossil. These results show that even for samples that have been intensely studied for decades, chemical information can be uncovered through detailed chemical imaging. Furthermore, imaging of the *Archaeopteryx* allowed several curatorial artifacts to be described in detail, including bone repair with bromine (Br)-rich epoxy (**Figure 12*a***) and the presence of numerous fingerprints around the periphery of the specimen, as revealed in Cl residue (**Figure 12*b***).

IR mapping, as discussed above, has also provided new insights into the preservation of soft tissue in fossilized organisms. High-resolution IR mapping and spectroscopy at synchrotron sources are producing a wealth of exciting new results in archeology (14, 15). In paleontology, recent research with a conventional IR source fitted with advanced mapping capabilities has shown that amide groups derived from original keratin within reptile skin can be detected (1, 2) and mapped to reveal skin structures with excellent resolution (2). The ability to nondestructively detect and map organic functional groups at low concentrations within precious fossils and archeological specimens is an extremely powerful development. However, the combination of FTIR and X-ray methodologies can provide even more exciting insights into preservation as well as about the original soft-tissue chemistry (2). **Figure 13** shows an exceptionally well preserved Eocene-age reptile skin bedding-plane fossil from the Green River Formation (~50 million years old, western United States). IR mapping with a raster-type contact attenuated total-reflectance methodology was used to analyze this specimen to determine whether the patterns held any useful chemical information.

Figure 14*a* presents an optical image of a skin molt taken from a living gecko, illustrating a structure dominated by distinct scales. The IR spectrum of β-keratin, the dominant component

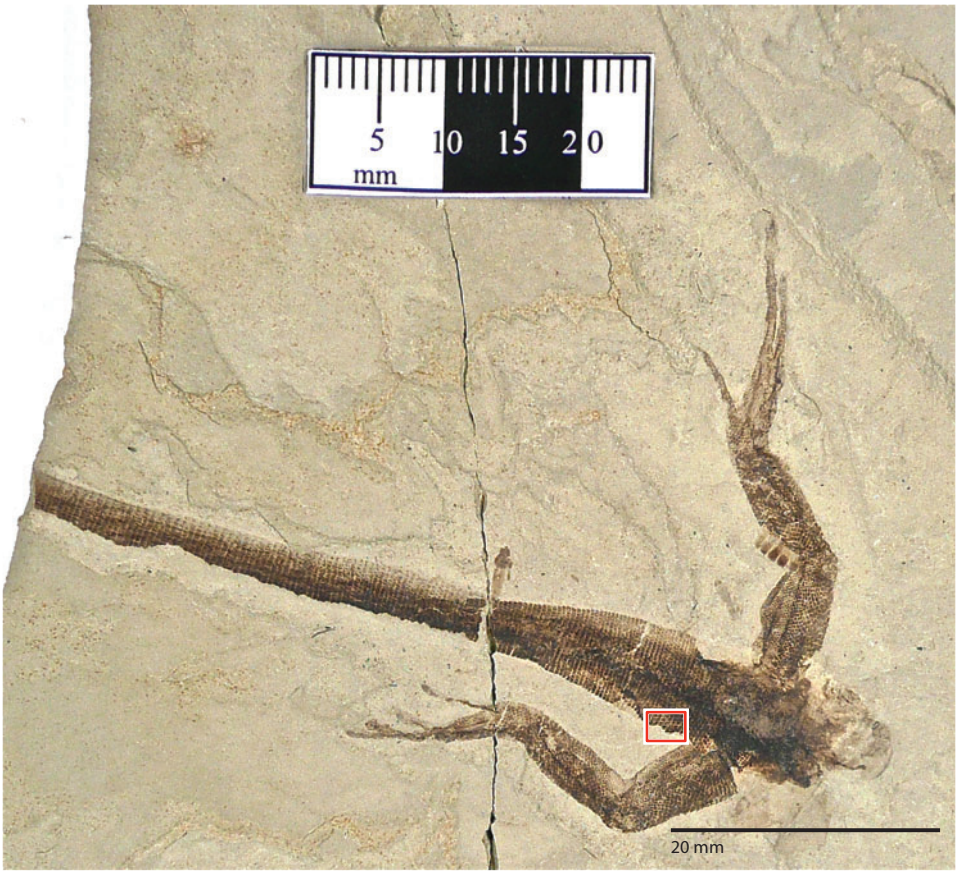

Figure 13

Exceptionally well preserved Eocene-age reptile skin from the Green River Formation, western United States. The red box shows the approximate location of the region mapped with Fourier transform IR spectroscopy. Adapted from Reference 2.

of reptile skin (42), shows strong absorption at wave numbers typical of the characteristic amide functional group (-CO-NH-C) in the structure of keratin. **Figure 14*b*** presents a map of the absorption intensity of the amide I band (C=O at 1,653 cm^{-1}) for the same region shown in **Figure 14*a***. The scale/hinge pattern is obvious in the FTIR image. In comparison, **Figure 14*c*,*d*** presents an optical image and an amide I map of the fossil skin. The amide I absorption intensity map in the fossil displays a pattern that is directly comparable to that of extant tissue. This result demonstrated that fossil soft-tissue components can be resolved and mapped on the basis of organic functional groups, raising a question as to whether element-specific SRS-XRF could also resolve details of chemical preservation or potentially provide insights into the biochemistry of the organism itself.

S levels are high (~7% by weight) in keratinous tissue, so the distribution of S within this fossil was an obvious target for SRS-XRF mapping, especially given the success of the FTIR analysis and the fact that thiol peaks were revealed in the spectra taken from the fossil skin. **Figure 15*a*** represents the first attempt at mapping S in this fossil; we simply mapped total S content by using an incident beam energy of 2,481.5 eV, above the S K-edge for sulfate. Because there are

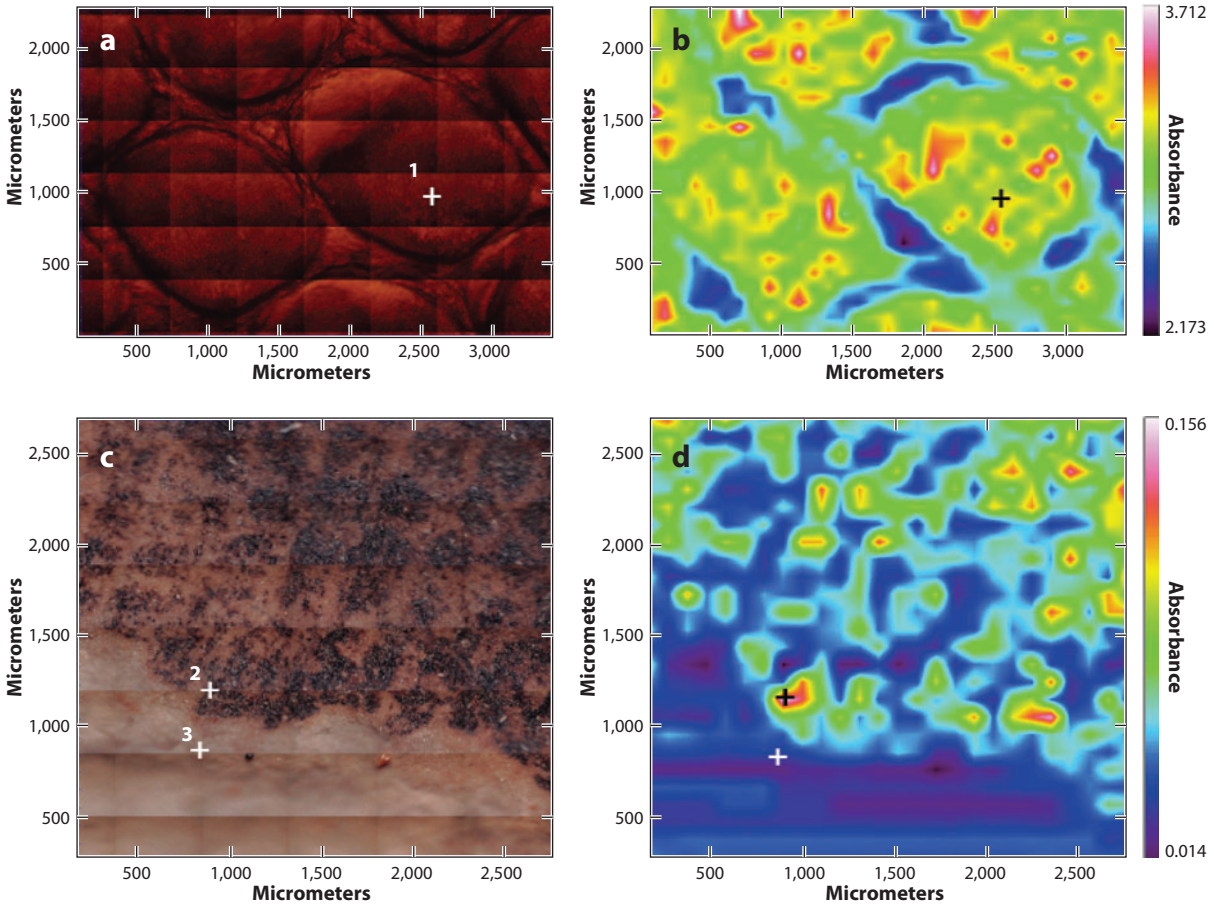

Figure 14

(*a*) Optical microscope image of extant reptile skin in transmitted light. (*b*) Map of absorption at 1,653 cm^{-1} in extant reptile skin (transmission mode). (*c*) Fossilized reptile skin in reflected light (boxed area in **Figure 13**). (*d*) Map of absorption at 1,653 cm^{-1} in fossilized skin (attenuated total-reflectance mode). The labeled crosshairs refer to point analyses; see Reference 2 for detailed spectra. Adapted from Reference 2.

evaporitic sulfate minerals on the bedding plane, this map is relatively featureless. We then selected several areas within the skin and collected XANES spectra at the S K-edge, showing that within the skin several reduced species of S could be resolved along with the inorganic sulfate. We then repeated the S map; this time, the incident beam was set below the critical excitation energy for sulfate but was high enough to excite the more-reduced organic S species. **Figure 15*b*** presents the results of this method. Note that the resolution of these maps is relatively poor because, in order to increase the low S signal, we needed to remove the pinhole and get as much flux onto the specimen as possible. Nonetheless, the second S map clearly shows that the organic S compounds are concentrated within discrete biological structures within the skin regions, consistent with the thiol peaks detected via FTIR and probably representing the residue of cleaved disulfide bonds derived from the original S-rich keratinous skin. In addition, we resolved trace-metal distribution patterns within the skin by using SRS-XRF. **Figure 16*a*** presents the distribution of Cu within the fossilized skin; **Figure 16*b*** compares this distribution with that of another trace

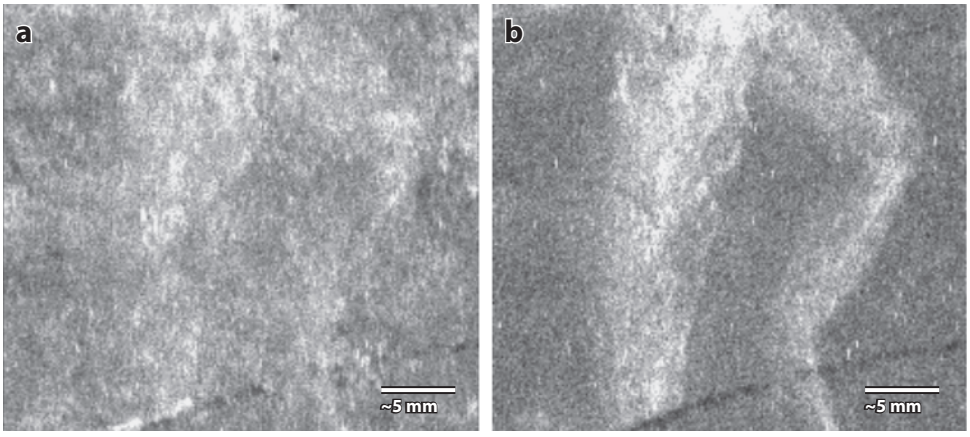

Figure 15

Synchrotron maps of S speciation in fossilized reptile skin (BHI-102B). (*a*) Synchrotron rapid scanning X-ray fluorescence (SRS-XRF) map (first method) of total S distribution on the specimen surface (incident beam energy 2,481.5 eV, above the sulfate-edge energy). (*b*) SRS-XRF map (second method) of organic S distribution within the specimen showing that nearly all the organic S is concentrated within the fossilized skin. This finding indicates that S species outside the fossil on the bedding plane are dominantly inorganic sulfate (incident beam energy, 2,479.9 eV; below the sulfate-edge energy). Adapted from Reference 2.

metal (Fe) within the extant skin of a gecko. Again, it is strikingly clear that the biological tissue controls the distribution and patterning of Cu within the fossil in a manner that is directly comparable to the metal distribution within the sample taken from a living reptile. This finding indicates that the metal inventory is endogenous. Because XANES spectroscopy at the K-edge of Cu does not show first-shell S, the Cu may be present either as an organic chelate solely within the skin or as a ternary complex bridging the surface oxygen sites of reactive minerals (such as analcime and smectite) with carboxylate or amide functional groups derived from skin compounds.

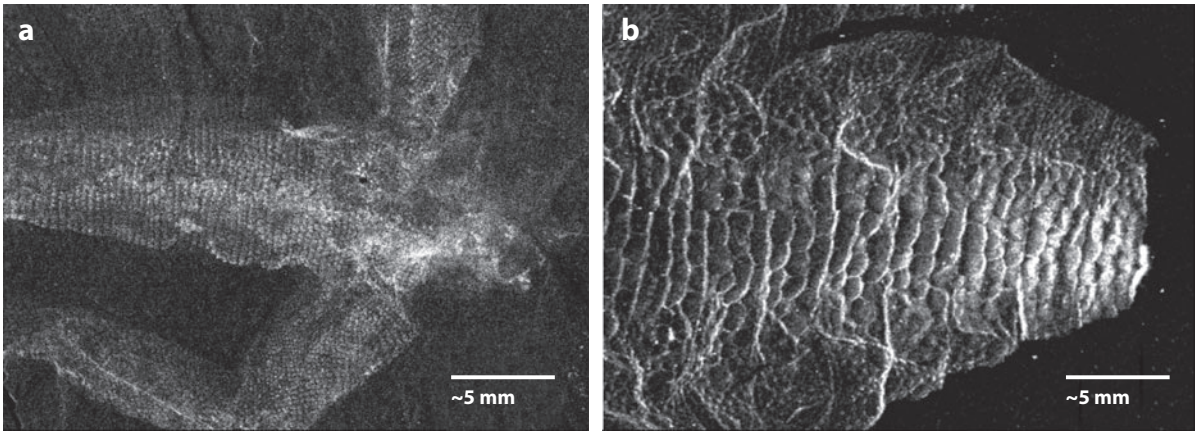

Figure 16

Synchrotron rapid scanning X-ray fluorescence maps of (*a*) Cu in fossilized reptile skin (BHI-102B) and (*b*) Fe in extant gecko skin. The maximum Fe concentration within the gecko skin is approximately 110 ppm. The fossilized skin has a comparable Cu concentration of approximately 180 ppm. Adapted from Reference 2.

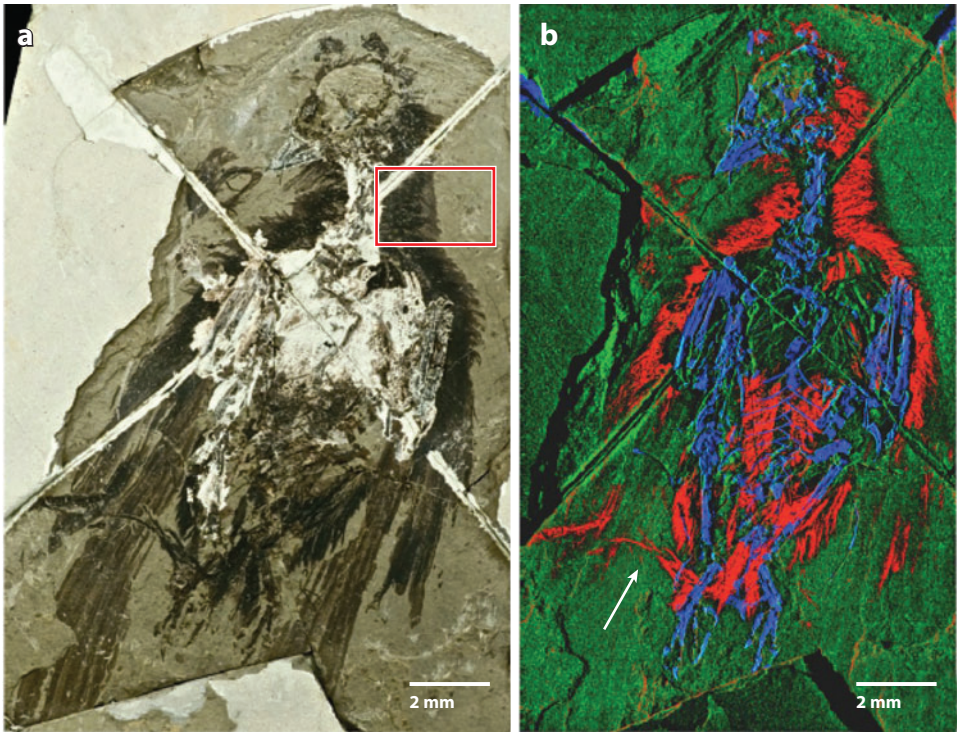

Figure 17

(*a*) An optical image of *Confuciusornis sanctus* (MGSF315). The red box shows the neck region discussed in detail in Reference 4. (*b*) Synchrotron rapid scanning X-ray fluorescence false-color images of the MGSF315 main slab. Elongated rectrices, which are characteristic of this species, are folded over and indicated by the white arrow. Red, Cu; blue, Ca; green, Zn. Adapted from Reference 4.

4.4. Confuciusornis sanctus and the Story of Color

Our final example shows that SRS-XRF can provide powerful new data for understanding the biochemistry of extinct organisms. Mapping not only uncovers patterns that give clues about the original chemistry but also highlights chemical hot spots (*a*) for detailed spectroscopic analysis by using the X-ray beam or (*b*) for the application of other techniques in a conservative manner. Color is an elusive but critically important feature of extinct organisms, and until recently it was nearly impossible to make robust conclusions about animal color with traditional methods. Feather color in birds stems mostly from chemical pigments, of which the most common are melanins (43). Resolving color patterns in extinct species may hold the key to understanding the selection processes in crucial evolutionary periods, and may help discern nonflight functions such as camouflage, communication, and sexual selection.

We were aware that the eumelanin pigment is a known chelator of a range of trace metals, so we targeted exceptionally well preserved fossils of critically important species to test whether metal chelate distributions could be resolved. In particular, *Confuciusornis sanctus* (Jehol Group, Lower Cretaceous, 131–120 Mya) occupies a key position in avian evolution; *C. sanctus* is the oldest documented species to display the derived avian beak (44). **Figure 17*a*** shows a visible-light image of one of the *C. sanctus* specimens analyzed; **Figure 17*b*** presents the distribution of the key trace metals Cu, Ca, and Zn within this specimen as a false-color intensity map. The

Figure 18

Artist's conception of eumelanin density in *Confuciusornis sanctus*, based on synchrotron rapid scanning X-ray fluorescence images. Adapted from Reference 4.

detail revealed in the distribution of Cu is striking and strongly implies that the Cu zoning is endogenous. Full EXAFS analysis of the Cu in the *C. sanctus* feather regions indicates that the element is organically bound, closely resembling the coordination environment found for Cu in natural melanin pigment. FTIR analysis of millimeter-sized flecks sampled from Cu-rich regions of this specimen produces spectra that are nearly identical to those from modern eumelanin pigment, and variable pressure-field emission gun SEM imaging at submicrometer resolution shows that fossilized microstructures resembling eumelanosomes are present in Cu-rich areas but absent elsewhere. Taken together, all of this evidence allowed us to conclude that the Cu distribution patterns in the feathers, which are also reproduced for Zn, Ca, and S, indicate that Cu is a reliable biomarker for the original distribution of eumelanin pigment within the original organism. **Figure 18** is an artist's conception of how the organism may have been shaded and is based on the trace-element densities recorded in the feathers.

Investigators provided further confirmation of this method by analyzing extant melanized soft tissues and looking for associated Cu anomalies. **Figure 19** compares visible-light images and SRS-XRF Cu maps for an extant squid and a fossilized squid. Both organisms show high concentrations of Cu associated with the eumelanin-rich ink sacks.

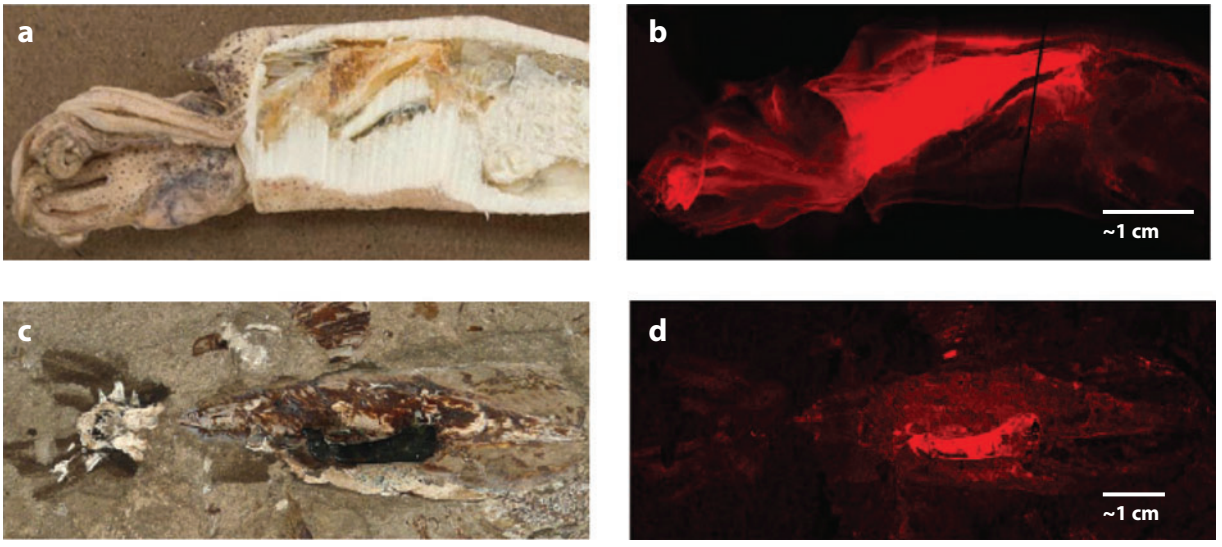

Figure 19

(*a*,*c*) Optical images. (*b*,*d*) Synchrotron rapid scanning X-ray fluorescence false-color images. (*a*,*b*) Sectioned extant squid. (*c*,*d*) Hakel fossil squid (BHI-2243B). Red coloring indicates Cu. The Cu zonation is controlled by biological structure, indicating eumelanin pigmentation.

5. THE FUTURE

We envision that the ability to combine nondestructive chemical mapping and quantitative chemical analysis with element-specific X-ray absorption analysis will allow the use of synchrotrons in paleontology and archeology to fuel a growing area of research over the next decade. Challenges will include improving the ability to image low–atomic weight elements and speeding up data acquisition of absorption spectra at key locations within samples. Here, current limitations are based not on the SR sources but rather on the detection, scanning, sample environment, and recording systems, in which progress is under way. We envision that synchrotron tomography and diffraction analysis will also fuel future beam-line development to optimize combined studies of structure and chemistry. Note that the use of synchrotron imaging on fossil specimens demonstrates that, in many cases, there is insufficient chemical data on modern organisms to enable full interpretation of results from fossils. For example, high-resolution mapping of modern bird feathers has not been widely performed. Consequently, the interpretation of fossilized feathers has required much effort in analyses of extant birds, which have influenced our understanding of modern species. In many ways, the use of SR in paleontology will contribute not only to our knowledge of the past but also to what we understand about the living world. The potential for these techniques to gently unravel the chemistry of long-extinct species and archeological finds is breathtaking. The possibility of mapping biosynthetic pathways, enzymatic reactions, the lost sentences of Greek philosophers, and the mass transfer of elements between organic and inorganic systems through deep time has much to offer many areas of science and the humanities. Advances in this multidisciplinary field will yield results far beyond archeology and paleontology.

DISCLOSURE STATEMENT

The authors are not aware of any affiliations, memberships, funding, or financial holdings that might be perceived as affecting the objectivity of this review.

ACKNOWLEDGMENTS

We thank all of our collaborators, the Stanford library, and the owners of the fossils and the Qur'ān palimpsest. The help of the staff at SLAC, in particular Martin George and Alex Garachtchenko, who were instrumental in developing the rapid scan system, is gratefully acknowledged. We are very grateful to the Black Hills Institute of Geological Research and the dedicated efforts of N.P. Edwards, H.E. Barden, W.I. Sellers, and P.L. Larson. Portions of this research were carried out at the Stanford Synchrotron Radiation Lightsource at SLAC National Accelerator Laboratory, a national user facility operated by Stanford University on behalf of the U.S. Department of Energy, Office of Basic Energy Sciences. The copyright of the manuscript images shown in **Figure 4** of this review is retained by the owner of the Archimedes Palimpsest.

LITERATURE CITED

1. Manning PL, Morris PM, McMahon A, Jones E, Gize A, et al. 2009. Preserved soft-tissue structures and organic molecules in a mummified hadrosaur dinosaur from the Hell Creek Formation, North Dakota (USA). *Proc. R. Soc. B* 276:3429–37
2. Edwards NP, Barden HE, van Dongen BE, Manning PL, Larson PL, et al. 2011. Infrared mapping resolves soft tissue preservation in 50-million-year-old reptile skin. *Proc. R. Soc. B* 278:3209–18
3. Bergmann U, Morton RW, Manning PL, Sellers WI, Farrar S, et al. 2010. *Archaeopteryx* feathers and bone chemistry fully revealed via synchrotron imaging. *Proc. Natl. Acad. Sci. USA* 107:9060–65
4. Wogelius RA, Manning PL, Barden HE, Edwards NP, Webb SM, et al. 2011. Trace metals as biomarkers for eumelanin pigment in the fossil record. *Science* 333:1622–26
5. Bergmann U. 2005. *X-Ray Fluorescence Imaging of the Archimedes Palimpsest: A Technical Summary*. Stanford: SLAC Natl. Accel. Lab. **http://www.slac.stanford.edu/gen/com/images/technical%20summary_final.pdf**
6. Bergmann U. 2007. Archimedes brought to light. *Phys. World* 9:39–42
7. Bergmann U, Knox K. 2009. Pseudo-color enhanced X-ray fluorescence imaging of the Archimedes palimpsest, document recognition and retrieval XVI. *Proc. SPIE* 7247:724702
8. Bergmann U. 2011. X-ray fluorescence. In *The Archimedes Palimpsest Publications*, ed. R Netz, W Noel, N Wilson, part III, ch. 4. Cambridge, UK: Cambridge Univ. Press
9. Sadeghi B, Bergmann U. 2010. The codex of a companion of the prophet and the Qur'ān of the prophet. *Arabica* 57:343–436
10. Larson NL, Morton RW, Larson PL, Bergmann U. 2010. A new look at fossil cephalopods. In *Cephalopods—Present and Past*, ed. K Tanabe, Y Shigeta, T Sasaki, H Hirano, pp. 303–14. Tokyo: Tokai Univ. Press
11. Dik J, Janssens K, van der Snickt G, van der Loeff L, Rickers K, Cotte M. 2008. Visualization of a lost painting by Vincent van Gogh using synchrotron radiation based X-ray fluorescence elemental mapping. *Anal. Chem.* 80:6436–42
12. Janssens K, Dik J, Cotte M, Susini J. 2010. Photon-based techniques for nondestructive subsurface analysis of painted cultural heritage artifacts. *Acc. Chem. Res.* 43:814–25
13. Monico L, van der Snickt G, Janssens K, De Nolf W, Miliani C, et al. 2011. Degradation process of lead chromate in paintings by Vincent van Gogh studied by means of synchrotron X-ray spectromicroscopy and related methods. 1. Artificially aged model samples. *Anal. Chem.* 83:1214–24
14. Cotte M, Dumas P, Taniguchi Y, Checroun E, Walter P, Susini J. 2009. Recent applications and current trends in cultural heritage science using synchrotron-based Fourier transform infrared microspectroscopy. *C. R. Phys.* 10:590–600
15. Reiche I, Lebon M, Chadefaux C, Müller K, Le Hô A, et al. 2010. Microscale imaging of the preservation state of 5,000-year-old archaeological bones by synchrotron infrared microspectroscopy. *Anal. Bioanal. Chem.* 397:2491–99
16. Manning PL. 2008. *Grave Secrets of Dinosaurs: Soft Tissues and Hard Science*. Washington, DC: Natl. Geogr.

17. Schweitzer MH. 2011. Soft tissue preservation in terrestrial Mesozoic vertebrates. *Annu. Rev. Earth Planet. Sci.* 39:187–216
18. Witmer LM. 1995. The extant phylogenetic bracket and the importance of reconstructing soft tissue in fossils. In *Functional Morphology in Vertebrate Paleontology*, ed. JJ Thomason, pp. 19–33. Cambridge, UK: Cambridge Univ. Press
19. Fraser RDB, MacRae TP. 1980. Molecular structure and mechanical properties of keratins. In *The Mechanical Properties of Biological Materials*, ed. JFV Vincent, JD Currey, pp. 211–46. Cambridge: Cambridge Univ. Press
20. Manning PL, Payne D, Pennicott J, Barrett P, Ennos RA. 2006. Dinosaur killer claws or climbing crampons? *Biol. Lett.* 2:110–12
21. Zhang FC, Kearns SL, Orr PJ, Benton MJ, Zhou Z, et al. 2010. Fossilized melanosomes and the colour of Cretaceous dinosaurs and birds. *Nature* 463:1075–78
22. Li Q, Gao K, Vinther J, Shawkey MD, Clarke JA, et al. 2010. Plumage color patterns of an extinct dinosaur. *Science* 327:1369–72
23. McNamara M, Orr PJ, Kearns SL, Alcala L, Anadon P, Penalver-Molla E. 2010. Organic preservation of fossil musculature with ultracellular detail. *Proc. R. Soc. B* 277:423–27
24. Johanson Z, den Blaauwen J, Newman M, Smith MM. 2010. No bones about it: An enigmatic Devonian fossil reveals a new skeletal framework—a potential role of loss of gene regulation. *Semin. Cell Dev. Biol.* 21:414–23
25. Winnick H, Doniach S. 1980. *Synchrotron Radiation Research*. New York: Plenum
26. Mimura H, Handa S, Kimura T, Yumoto H, Yamakawa D, et al. 2010. Breaking the 10 nm barrier in hard X-ray focusing. *Nat. Phys.* 6:122–25
27. Yan H, Rose V, Shu D, Lima E, Kang HC, et al. 2011. Two dimensional hard X-ray nanofocusing with crossed multilayer Laue lenses. *Opt. Express* 19:15069–76
28. Popescu BFG, George MJ, Bergmann U, Garachtchenko AV, Kelly ME, et al. 2009. Mapping metals in Parkinson's and normal brain using rapid-scanning X-ray fluorescence. *Phys. Med. Biol.* 54:651–63
29. Popescu BFG, Robinson CA, Chapman LD, Nichol H. 2009. Synchrotron X-ray fluorescence reveals abnormal metal distributions in brain and spinal cord in spinocerebellar ataxia: a case report. *Cerebellum* 8:340–51
30. Popescu BFG, Robinson CA, Rajput A, Rajput AH, Harder SL, Nichol H. 2009. Iron, copper, and zinc distribution of the cerebellum. *Cerebellum* 8:74–79
31. Hopp K, Popescu BFG, McCrea RPE, Harder SL, Robinson CA, et al. 2010. Brain iron detected by SWI high pass filtered phase calibrated with synchrotron X-ray fluorescence. *J. Magn. Reson. Imaging* 31:1346–54
32. Lee PA, Citron PH, Eisenberger P, Kincaid BM. 1981. Extended X-ray absorption fine structure—its strengths and limitations as a structural tool. *Rev. Mod. Phys.* 53:769–806
33. Rehr JJ, Albers RC. 2000. Theoretical approaches to X-ray absorption fine structure. *Rev. Mod. Phys.* 72:621–54
34. Perrichot V, Marion L, Néraudeau D, Vullo R, Tafforeau P. 2008. The early evolution of feathers: fossil evidence from Cretaceous amber of France. *Proc. R. Soc. B* 275:1197–202
35. Sellers WI, Manning PL. 2007. Estimating maximum running speeds using evolutionary robotics. *Proc. R. Soc. B* 274:2711–16
36. Darwin C. 1859. *On the Origin of Species by Means of Natural Selection, or the Preservation of Favoured Races in the Struggle for Life*. London: Murray
37. Wellnhofer P. 2009. Archaeopteryx*: The Icon of Evolution*. Berlin: Springer. 208 pp.
38. Buckley M, Larkin N, Collins M, Collins MJ. 2011. Mammoth and mastodon collagen sequences: survival and utility. *Geochim. Cosmochim. Acta* 75:2007–16
39. Schweitzer MH, Suo Z, Avci R, Asara JM, Allen MA, et al. 2007. Analyses of soft tissue from *Tyrannosaurus rex* suggest the presence of protein. *Science* 316:277–80
40. Buckley M, Walker A, Ho SYW, Yang Y, Smith C, et al. 2008. Comment on "Protein sequences from Mastodon and *Tyrannosaurus rex* revealed by mass spectrometry." *Science* 319:33
41. Koenig AE, Rogers RR, Trueman CN. 2009. Visualizing fossilization using laser ablation–inductively coupled plasma–mass spectrometry maps of trace elements in Late Cretaceous bones. *Geology* 37:511–14

42. Alibardi L, Toni M. 2006. Cytochemical, biochemical, and molecular aspects of the process of keratinization in the epidermis of reptilian scales. *Prog. Histochem. Cytochem.* 40:73–134
43. Simon JD, Peles D, Wakamatsu K, Ito S. 2009. Current challenges in understanding melanogenesis: bridging chemistry, biological control, morphology, and function. *Pigment Cell Melanoma Res.* 22:563–79
44. Hou LH, Martin LD, Zhou ZH, Feduccia A, Zhang FC. 1999. A diapsid skull in a new species of the primitive bird *Confuciusornis*. *Nature* 399:679–82

Annual Review of
Analytical Chemistry

Volume 5, 2012

Contents